XLVI CILAMCE
VITÓRIA - ES - BRAZIL - 2025
XLVI IBERO-LATIN AMERICAN CONGRESS ON COMPUTATIONAL METHODS IN ENGENEERING

Stochastic Assessment of the Influence of Neighboring Buildings on the Drag Force of a Building

Gregório Sandro Vieira[1], José Luis Vital de Brito[2]

[1]*Faculdade de Engenharia Civil - PPGEC, Federal University of Uberlândia*
Av. João Naves de Ávila, 2121 Campus Santa Mônica - Bloco 1Y, CEP: 38400-902, MG/Uberlândia, Brasil
gregorio.vieira@ufu.br
[2]*Dept. of Civil and Environmental Engineering - PECC, University of Brasília*
Faculdade de Tecnologia, Bloco E, Asa Norte, CEP 70.910-900, DF/Brasília, Brasil
jlbrito@unb.br

Abstract.

Urban verticalization has intensified the construction of high-rise buildings in areas with low vertical density, where the presence of adjacent structures can significantly affect wind loads — especially the drag force. This study presents a stochastic evaluation of how neighboring buildings influence the drag force acting on a target structure, based on wind tunnel test data. Drag forces were calculated for five configurations: one isolated and four with varying neighboring arrangements. Statistical descriptors (variance, standard deviation, RMS) and stochastic quantifiers (Hellinger distance, Kullback-Leibler divergence, and perturbation index $\Delta\beta$) were used to assess the differences. The Anderson-Darling test was applied to identify the most suitable probability distribution for each case. Comparative results between two principal wind directions (0° and 90°) highlight the aerodynamic disturbances caused by neighboring buildings, supporting the importance of considering urban context in structural wind load evaluations.

Keywords: Wind Load Disturbance, Surrounding Buildings, Urban Wind Effects

1 Introduction

Population growth, the high value of land in central urban areas, increasing occupation of these regions, and the natural expansion of metropolitan zones have led to the construction of large-scale buildings in areas that were previously undeveloped or occupied by low-rise structures. In such contexts, the initial design assumptions for these pioneering buildings typically consider wind acting freely on all façades. However, over time, it is natural for new buildings of similar height and scale to be erected nearby.

Blessmann [1] states that the presence of surrounding obstacles alters the wind flow pattern, resulting in changes in the pressure distribution on a building's façades. A direct consequence of this aerodynamic interference is the modification of the drag force acting on the structure. Depending on the relative positioning and geometry of nearby buildings, such interactions may attenuate or amplify the wind-induced forces and moments. In some cases, this may lead to values that exceed the limits prescribed by design standards, as noted by Vieira [2], [3], [4], and other researchers.

In this context, the present study aims to stochastically evaluate the behavior of wind flow around a standard tall building, considering the influence of a neighboring structure of similar size located in close proximity. For this purpose, experimental data obtained by Vieira [2] through wind tunnel tests were used. Based on these data, a probabilistic analysis of the drag force acting on the building was carried out, both in an isolated condition and in the presence of different neighboring configurations. To support the comparative evaluation of these effects, the Monte Carlo Method was applied, and a drag force perturbation index was determined, quantifying the variations associated with aerodynamic interference between structures.

2 Theoretical review

One of the key parameters to be considered when evaluating wind action on a building is the drag force. According to ABNT-NBR6123:2023 [6], this force corresponds to the component of the wind load acting in the same direction as the flow and is calculated using eq. (1). The calculation takes into account the dynamic pressure (q), the drag coefficient (C_a), the effective frontal area (A_f), and the shelter factor or neighboring interference factor (f_v).

$$F_a = q\, C_a\, A_e\, f_v. \tag{1}$$

An alternative to obtaining more accurate values of the drag force, instead of relying solely on the expressions prescribed by standards, is to conduct experimental tests that provide more representative data regarding wind action. In such tests, depending on the geometry of the model, several pressure tap points are defined—these are the primary measurements recorded by the instruments. During the data acquisition period, multiple readings are collected, which, depending on the type of study, can be analyzed in various ways.

Certain statistical analyses are particularly useful when processing data from wind tunnel experiments, such as the time-averaged mean, variance and standard deviation.

It is not always feasible to carry out multiple experiments to achieve specific key results. In such cases, a wind tunnel test can be considered an ergodic process, in which a single experiment is sufficient to adequately represent the stochastic behavior under analysis. For this type of process, the discrete time average tends to the expected (mean) value. The eq. (2) represents this discrete time average for a discrete-time stochastic process.

$$\overline{x} = \frac{1}{n}\sum_{i=1}^{n} x_i. \tag{2}$$

Another important parameter to be considered is the variance, represented by eq. (3), which quantifies the dispersion of the data around the mean. Statistically, the variance represents the average of the squared deviations of the data from the sample mean, and is calculated as follows:

$$Var(x) = \frac{1}{n-1}\sum_{i=1}^{n}(x_i - \overline{x})^2. \tag{3}$$

A more intuitive parameter—since it operates on the same scale as the data—is the standard deviation, which is simply the square root of the variance, as shown in eq. (4):

$$\sigma = \sqrt{Var(x)} = \sqrt{\frac{1}{n-1}\sum_{i=1}^{n}(x_i - \overline{x})^2}. \tag{4}$$

To determine which curve best represents the distribution of data collected in an experiment, a goodness-of-fit test can be applied, such as the Anderson–Darling (eq. (5)), Kolmogorov–Smirnov (eq. (6)), or Chi-squared (eq. (7)), among others. These tests assess the agreement between the empirical data distribution and theoretical distributions such as normal, exponential, and lognormal.

$$A^2 = -n - \frac{1}{n}\sum_{i=1}^{n}\left[(2i-1)\cdot\left(\ln F(X_i) + \ln\left(1 - F(X_{n+1-i})\right)\right)\right]. \tag{5}$$

$$D_n = \sup_x \left|F_n(x) - F(x)\right|. \tag{6}$$

$$\chi^2 = \sum_{i=1}^{k} \frac{(O_i - E_i)^2}{E_i}. \tag{7}$$

In addition to identifying the most appropriate distribution for the data, goodness-of-fit tests also support the validation of statistical models that rely on assumptions regarding the underlying variable distributions. The results of these tests are typically interpreted based on the *p*-value, which, if below a predefined significance level (commonly 5%), leads to the rejection of the null hypothesis that the data follow the tested distribution.

It is important to consider the sample size and the desired sensitivity when selecting a test. For example, the Shapiro-Wilk test is particularly suitable for small sample sizes, whereas the Anderson-Darling test is more sensitive to discrepancies in the tails of the distribution. This sensitivity is especially relevant in studies involving statistical extremes, such as structural safety analyses.

To model the probabilistic behavior of physical phenomena and support statistical comparisons between scenarios, the Monte Carlo method is often employed. This technique allows for the generation of large sets of random samples from fitted probability distributions, enabling the estimation of probabilistic events of interest. For example, let $C_{ref} \sim f_1(c)$ and $C_{pert} \sim f_2(c)$ represent random variables describing a given response (e.g., aerodynamic force) under reference and perturbed conditions, respectively. A performance function can be defined by eq. (8):

$$g(c) = C_{ref} - C_{pert}. \tag{8}$$

The probability of perturbation is defined by eq. (9):

$$P_{pert} = P(g(c) \leq 0) = P(C_{ref} \leq C_{pert}). \tag{9}$$

Such a formulation is relevant in contexts where the relative magnitude of two stochastic responses must be assessed—such as comparing aerodynamic loads in isolated versus urban-influenced conditions.

Finally, to synthetically represent changes in the stochastic behavior at a specific point on the structure, the Perturbation Index, denoted as $\Delta\beta$ (eq. (10)), is employed. This index is a scalar metric that quantifies the impact of external interferences—such as the presence of neighboring buildings—on the probabilistic distribution of experimentally observed data. It is commonly derived from the perturbation probability by applying the inverse of the standard normal cumulative distribution function, as follows:

$$\Delta\beta = \Phi^{-1}(1 - P_{pert}). \tag{10}$$

Alternatively, it can be formulated using divergence-based quantifiers such as the total variation distance, Kullback-Leibler divergence, or Hellinger distance. The value of $\Delta\beta$ provides a direct indication of the degree of change in the local stochastic response. Higher values indicate greater sensitivity to perturbations, making this index a valuable tool in risk assessment, urban wind design, and studies aimed at mitigating undesirable aerodynamic effects in the built environment.

3 Methodology

3.1 Experimental Study

This study adopted as its reference model the standardized building developed by the Commonwealth Advisory Aeronautical Research Council (CAARC). For this reason, it is customary to refer to it simply as the "CAARC building", a convention that will be followed throughout this work. The use of this model allows for the implementation of experimental procedures similar to those employed in laboratories worldwide and facilitates the comparison of data and results from various studies on building aerodynamics. The CAARC model (Figure 1) consists of a prismatic structure with a rectangular cross-section, representing a building with dimensions of

30.48 m × 45.72 m × 182.88 m. As with the primary building under investigation, the models used to simulate the surrounding structures also followed the CAARC building dimensions.

In the building under study, pressure measurements were carried out on all four façades, at ten different levels. Based on these values, the forces acting on the influence areas associated with each pressure tap were calculated. From these forces, the drag force acting on the building was determined according to the wind direction. In addition to analyzing the building in isolation, the study also considered the presence of a neighboring building of the same height, positioned in front of the main building in four different configurations, as illustrated in Figure 2, where 'H' represents the height of the analyzed building.

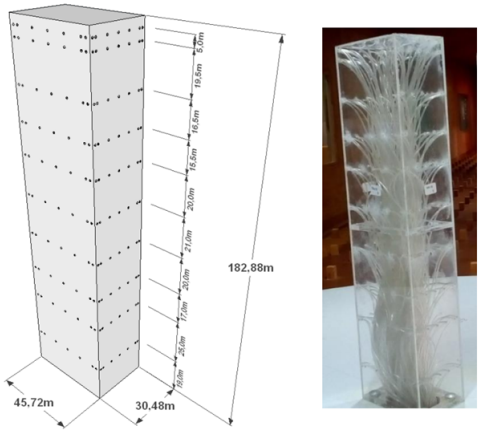


Figure 1. CAARC Building Model

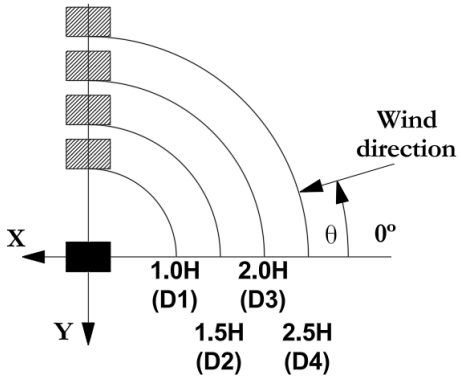


Figure 2. Positioning of neighboring buildings

Based on the collected experimental data, the resultant drag forces acting on the building façades were calculated for wind directions of 0° and 90°, as prescribed by the Brazilian standard and commonly adopted in most international wind load codes. For each scenario, the resultant drag force was calculated from point pressure measurements following standardized mathematical procedures.

Key descriptive statistics of the drag forces, including mean, variance, and standard deviation, were obtained in accordance with the methodology employed by Villoslada et al. [5]. Additionally, to ensure the statistical modeling validity, the data were subjected to goodness-of-fit tests against Normal, Lognormal, and Weibull theoretical distributions, using the Anderson-Darling test, complemented by Kolmogorov-Smirnov and Chi-square tests.

Based on the fitted distributions, Monte Carlo simulations with one million samples per case were performed to estimate the aerodynamic perturbation probabilistic index, denoted as the coefficient $\Delta\beta$. The analysis included the generation of probability density function plots for each condition, enabling a comparative evaluation between the isolated case and configurations with neighboring buildings.

4 Results and analysis

As shown in the data presented in Table 1, even when the neighboring buildings are not aligned with the building under study and the wind direction, but are positioned laterally, they still exert an influence on the drag force, increasing its magnitude. The building positioned at distance D1 induced an increase of nearly 23%, representing the most significant impact on the drag force. In the other positions, increases ranging from 5% to 15% were observed.

In addition to the increase in the mean drag force, the presence of neighboring buildings also affects the variability of the measurements. In case V1D1, although the highest mean increase was observed (approximately 23%), both the variance and the standard deviation were significantly lower compared to the isolated case, indicating a more uniform response throughout the readings. Conversely, configurations V1D2 and V1D3 exhibited substantially higher variances and standard deviations, suggesting more pronounced fluctuations in the drag force, possibly associated with unstable aerodynamic effects induced by the position of the neighboring buildings. Case V1D4 also showed a considerable mean increase, accompanied by elevated variability, although lower than that observed in V1D2 and V1D3. These results indicate that not only the mean magnitude but also the dispersion of the forces should be considered when assessing the influence of surrounding buildings.

Table 1. Drag Force Data - 0º Wind Direction

Test	Average (kN)	Variance	Standard Deviation (kN)
Isolated	2237,9	71955,0	268,2
V1D1	2750,3	38689,3	196,7
V1D2	2361,9	101876,8	319,2
V1D3	2576,4	100884,3	317,6
V1D4	2573,9	87792,2	296,3

As shown in Table 2, the presence of neighboring buildings markedly influenced the drag force. In this configuration, the influence was predominantly characterized by a reduction in the mean drag force when compared to the isolated case. The largest reduction was observed in case V1D1, where the mean force decreased by approximately 90%, followed by V1D2, with a reduction of around 83%. Configurations V1D3 and V1D4 exhibited less pronounced reductions, of approximately 57% and 52%, respectively.

In addition to changes in the mean values, notable variations in force dispersion were also recorded. All perturbed configurations showed higher variances and standard deviations compared to the isolated case, indicating greater fluctuations in the measured drag forces. This effect was most pronounced in cases V1D2 and V1D3, which exhibited both significant mean reductions and elevated variability, suggesting that the aerodynamic interference from lateral neighboring buildings may have induced unsteady and turbulent flow patterns. These findings reinforce the importance of jointly evaluating both the magnitude and variability of aerodynamic loads when assessing the influence of surrounding buildings on structural wind response.

Table 2. Drag Force Data - 90º Wind Direction

Test	Average (kN)	Variance	Standard Deviation (kN)
Isolado	4730,3	231227,2	480,9
V1D1	470,4	261945,8	511,8
V1D2	800,6	335738,7	579,4
V1D3	2034,5	389877,0	624,4
V1D4	2277,1	292016,7	540,4

As evidenced in Figure 3 and the data presented in Table 1, the presence of neighboring buildings, even when positioned laterally to the studied building and to the wind direction, significantly altered the drag force. In the V1D1 case, with the neighboring building located at a distance of 1.0 H, the largest shift of the probability density

distribution toward higher values was observed, with an average increase of approximately 512 kN compared to the isolated case, along with reduced overlap between distributions, indicating a high probability of perturbation. For V1D2 (1.5 H), the average increase was small, and the overlap was greater, suggesting a lower aerodynamic effect. In V1D3 (2.0 H) and V1D4 (2.5 H), relevant average increases and amplified variability were observed, with V1D3 showing the highest standard deviation (624.4 kN), indicating greater flow instability. These results suggest that the impact of neighboring buildings does not follow a monotonic trend with distance, with specific configurations such as V1D1 and V1D3 exhibiting more pronounced interference, possibly due to channeling effects and vortex interactions in the building's surroundings.

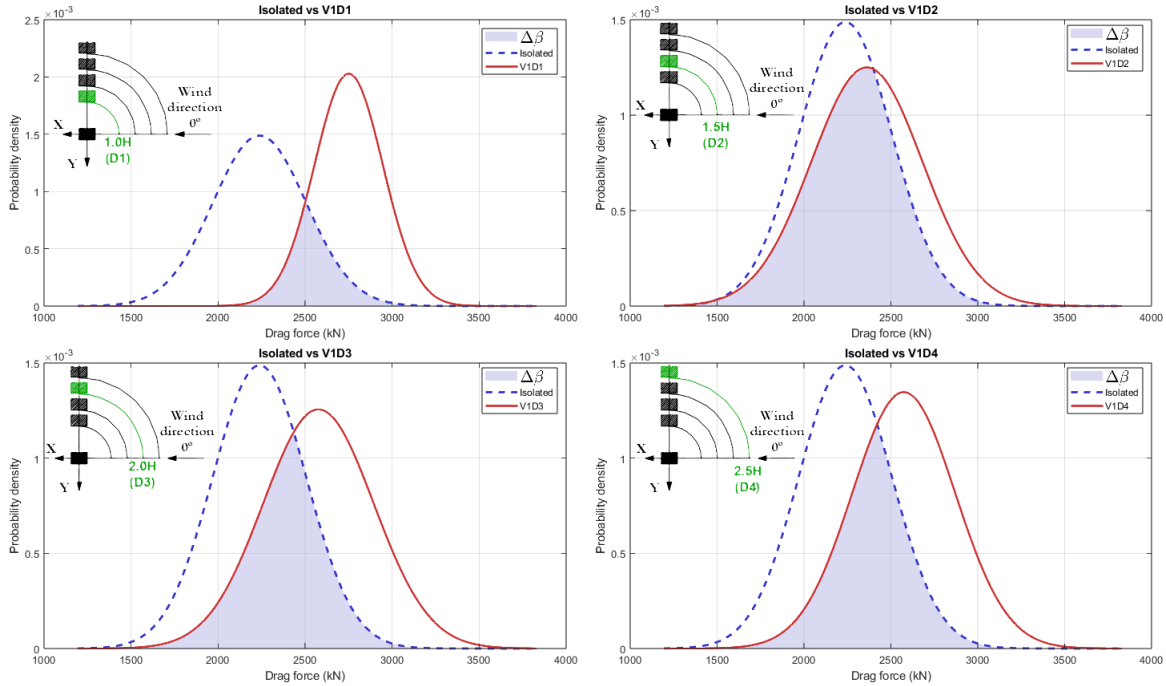


Figure 3. Pairwise Comparison of Densities with Overlay Shading - 0°direction

The analysis of Figure 4 shows that the presence of a neighboring building laterally induces a significant reduction in drag force compared to the isolated case, with the probability density distributions shifting toward lower values across all examined spacings (from 1.0H to 2.5H). This effect is most pronounced in the V1D1 configuration (spacing of 1.0H), where the distribution is tightly concentrated near zero, indicating strong flow blockage. As the spacing increases (from 1.5H to 2.5H), there is a gradual shift toward higher—though still below isolated—drag values, accompanied by greater dispersion, likely due to reduced turbulent interactions. These findings suggest that aerodynamic interference from the neighboring building is nonlinear, peaking at the closest spacing (1.0H) but remaining significant even at 2.5H. This underscores the importance of accounting for wake effects in wind load assessments within urban environments.

5 Conclusions

The results demonstrate that laterally positioned neighboring buildings significantly influence the drag force on the studied building, affecting both mean magnitude and variability. The impact varies nonlinearly with spacing, with the closest configuration (V1D1 at 1.0H) causing the largest changes—either increasing drag by up to 23% with reduced variability or decreasing it by up to 90% with increased fluctuations, depending on flow conditions.

Intermediate distances (1.5H to 2.5H) exhibit less pronounced but still notable effects, including increased variability and complex aerodynamic interactions such as vortex shedding and flow channeling. Probability density analyses confirm that wake interference remains significant up to 2.5H spacing, underscoring the need to consider both mean and statistical dispersion of wind loads in urban wind engineering.

These findings highlight the complex, nonlinear nature of aerodynamic interference from lateral buildings

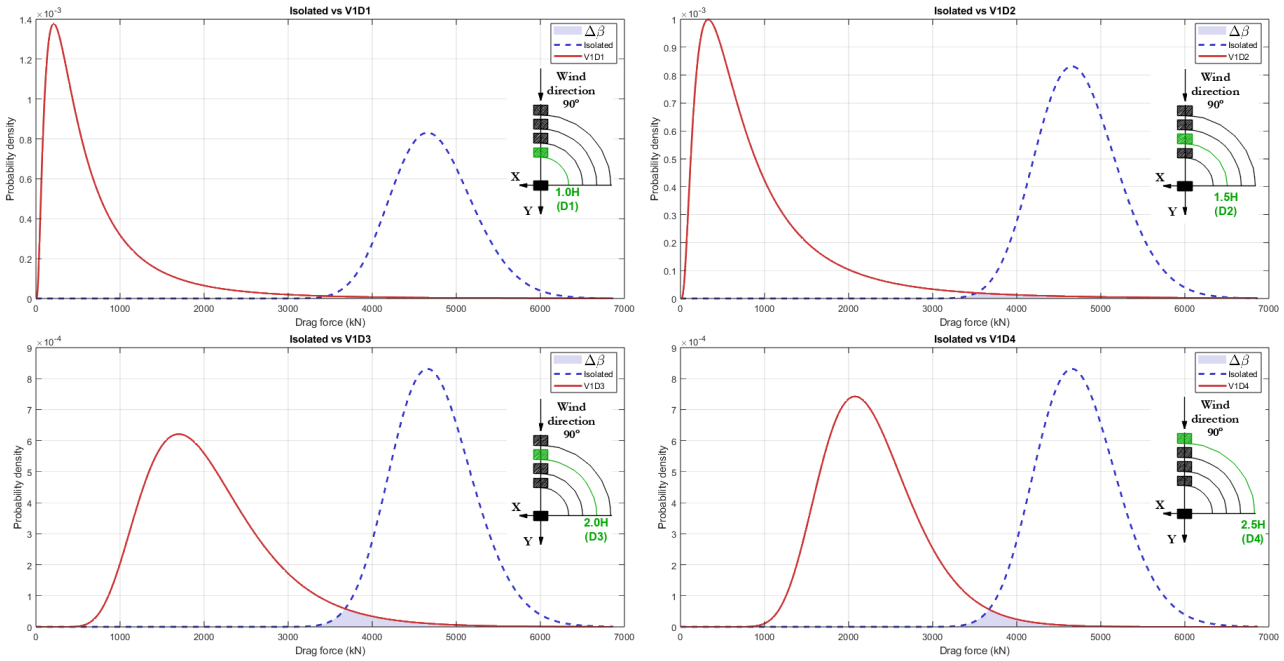


Figure 4. Pairwise Comparison of Densities with Overlay Shading - 90°direction

and the necessity for detailed assessments to ensure accurate structural wind load predictions in dense urban environments.

Acknowledgements. The authors would like to thank the National Council for Scientific and Technological Development (CNPq) for supporting this research. The authors also acknowledge the Graduate Program in Civil Engineering at the Federal University of Uberlândia (PPGEC-UFU), and the Graduate Program in Structural and Civil Construction Engineering at the University of Brasília (PECC-UnB), for their institutional support.

Authorship statement. The authors hereby confirm that they are the sole liable persons responsible for the authorship of this work, and that all material that has been herein included as part of the present paper is either the property (and authorship) of the authors, or has the permission of the owners to be included here.

References

[1] J. Blessmann. *O vento na engenharia estrutural*. UFRGS, 2013.
[2] G. S. Vieira. *Estudo Experimental dos Esforços Solicitantes em um Edifício Alto Devidos à Ação do Vento Considerando a Influência de Edificações Vizinhas*. Universidade de Brasília, Tese, 2016.
[3] G. S. Vieira, de J. L. V. Brito, and A. M. LOREDO-SOUZA. Experimental study on the interference intensity produced by the presence of neighboring buildings in the wind action in a tall building. *IBRACON Structures and Materials Journal*, vol. 11, pp. 1036–1052, 2018a.
[4] G. S. Vieira, de J. L. V. Brito, and A. M. LOREDO-SOUZA. Experimental study of the neighborhood effects on the mean wind loading over two equivalent high-rise buildings. *Latin American Journal of Solids and Structures*, vol. 15, pp. 1–15, 2018b.
[5] G. Villoslada, T. F. A. Lavôr, de J. L. V. Brito, and J. C. Pantoja. Determination of the drag force disturbance index for analysis of neighborhood effect in tall buildings subject to wind. *Proceedings of the joint XLV Ibero-Latin-American Congress on Computational Methods in Engineering - ABMEC*, vol. , 2024.
[6] ABNT-NBR6123:2023. *Forças devidas ao vento em edificações*. Associação Brasileira de Normas Técnicas, Rio de Janeiro, 2023.